Article Type: Letter

Title: Higher methanotroph abundance and bottom-water methane in ponds with floating photovoltaic arrays

Running head: Floating solar and methane in ponds

Author Names: Nicholas E. Ray[1], Sophia Aredas[2], Steven M. Grodsky[3], Ash Canino[4], Simone J. Cardoso[5], Meredith A. Holgerson[6], Meredith Theus[6], Marian L. Schmidt[2]

Author Affiliations:
[1] School of Marine Science & Policy, University of Delaware, USA
[2] Department of Microbiology, Cornell University, USA
[3] U.S. Geological Survey, New York Cooperative Fish and Wildlife Research Unit, Department of Natural Resources and the Environment, Cornell University, USA
[4] Department of Natural Resources and Environment, Cornell University, USA
[5] Department of Zoology, Institute of Biological Sciences, Universidade Federal de Juiz de Fora, Brazil
[6] Department of Ecology and Evolutionary Biology, Cornell University, USA

Corresponding Author: Nicholas E. Ray; nickray@udel.edu

Author Contribution Statement:
NER designed the study, provided supplies, performed field sampling, laboratory analyses, and data analysis, and wrote the first draft of the manuscript. SMG secured funding, constructed the floating solar arrays, performed field sampling, and edited the manuscript. AC, SJC, and MT performed field sampling and edited the manuscript. MAH secured funding, performed field sampling, and edited the manuscript. SA performed field sampling, laboratory analyses, data analysis, and edited the manuscript. MLS designed the study, provided supplies, data analysis, secured funding, and edited the manuscript.

Scientific Significance Statement (125 word max)

Producing energy using floating photovoltaic (FPV) powerplants offers an opportunity to produce renewable energy, spare land, and reduce evaporation from ponds, lakes, and reservoirs. However, FPV deployment in these ecosystems is associated with colder temperatures, less oxygen availability, and changes in carbon cycling processes. Specifically, experimental evidence demonstrates an increase in concentrations of methane – a potent greenhouse gas – in ponds following FPV deployment. In this study, we investigate how microbial communities associated with aquatic methane cycling differ between ponds with and without FPV. We show that FPV deployment increases bottom-water methane concentrations and triggers dense blooms of methane-oxidizing bacteria. These results provide the first evidence that microbial communities respond strongly to engineered shading and may help buffer greenhouse gas emissions in solar-covered waters.

Data and Code Availability

All raw and processed data for this project are publicly available. The code used for statistical comparisons, generating figures, and processing microbial community data are available on GitHub at https://github.com/MarschmiLab/Ray_LO_Letters_FPV_Methane. Biogeochemical data and summaries of methane cycling microbe abundances is available for download via the Figshare Repository (https://doi.org/10.6084/m9.figshare.29614025.v1). The raw, compressed 16S rRNA gene sequencing fastq files are available in the NCBI Sequence Read Archive (SRA) under the BioProject accession number PRJNAXXXXXXX (This will be made available upon acceptance or by reviewer request). All flow cytometry data are available in the Flow Repository database with the ID number XXXXX (This will be made available upon acceptance or by reviewer request).

Abstract (150 words max)

Floating photovoltaic (FPV) arrays alter the biogeochemistry of waterbodies on which they are deployed. Here, we investigated dissolved methane (CH_4) dynamics and associated CH_4 cycling microbial communities in the second-year of FPV deployment (70% aerial coverage) in experimental ponds. We found that bottom-water CH_4 concentrations were twice as high in ponds with FPV compared to those without. Surface water CH_4 concentrations were orders of magnitude lower than bottom-waters, but were similar between ponds with and without FPV. There were no differences in potential sediment CH_4 production or CH_4 associated microbes. Instead, dissolved CH_4 patterns could be explained by elevated abundance of methanotrophic bacteria in the water column of FPV ponds, where late-summer abundances exceeded 1,000,000 cells mL^{-1}. Prolonged periods of CH_4 production in low oxygen FPV ponds likely favored blooms of methanotrophs in surface waters where some oxygen is available, mitigating diffusive CH_4 emissions to the atmosphere following FPV deployment.

Keywords: pond, methane, floating solar, greenhouse gas, methanogen, methanotroph

Introduction

Methane (CH_4) emissions from aquatic ecosystems have increased because of human activity (Jackson et al. 2024). Floating photovoltaic arrays (FPV), first deployed in 2007, are a rapidly expanding renewable energy technology that can alter aquatic CH_4 dynamics and emissions (Cazzaniga and Rosa-Clot 2021; Ray et al. 2024). By 2023, over 643 FPV power plants had been installed on lakes, ponds, and reservoirs worldwide (Nobre et al. 2024; Ramanan et al. 2024). There is substantial interest and potential in expanding FPV use on reservoirs and lakes to meet demands for renewable energy (Jin et al. 2023; Woolway et al. 2024), but the ecological and biogeochemical tradeoffs – particularly effects on CH_4 cycling – must be evaluated before broader deployment (Almeida et al. 2022; Gallaher et al. 2025).

FPV deployment is associated with lower water temperatures (Dörenkämper et al. 2021; Andini et al. 2022), reduced oxygen availability (Wang et al. 2022; Ray et al. 2024), and changes in stratification (Ilgen et al. 2023). These factors influence CH_4 dynamics in small, shallow systems where FPV has most commonly been deployed (Bastviken et al. 2004; Aben et al. 2017; Ray and Holgerson 2023; Nobre et al. 2024). Indeed, in the first year of FPV deployment, experimental ponds with FPV showed twice the dissolved CH_4 concentrations and CH_4 ebullition compared to control ponds, but diffusive CH_4 emissions were lower (Ray et al. 2024). Whether these observed patterns persist over time or might be similar in other ecosystems is unclear.

Understanding how FPV alters CH_4 cycling microbes may reduce uncertainty in CH_4 emission responses. Methanogenic archaea (CH_4 producers) and methanotrophic bacteria (CH_4 consumers) regulate CH_4 fluxes, but it remains unresolved how FPV-induced changes in

temperature, light, oxygen, and primary production affect their abundance, composition, and activity. Evidence from non-FPV settings suggests these conditions will re-structure CH4 cycler communities and alter metabolic rates (Wang et al. 2021; Bertolet et al. 2022). Clarifying microbial responses to FPV is critical for predicting whether this technology amplifies or dampens CH_4 emissions and, more broadly, can inform how pond microbial communities respond to reduced light and oxygen.

Here, we investigate how FPV affects CH_4 dynamics in temperate experimental ponds during the second year of FPV deployment. We pair observations of temperature, dissolved oxygen, dissolved CH_4, and the CH_4-associated microbial community throughout the summer with CH_4 process rates during an intensive mid-summer sampling campaign in ponds with and without FPV. Because methanotrophs can be challenging to resolve via 16S alone, we focus on well-characterized CH_4 oxidizers and pair community data with functional rate measurements to capture both composition and activity.

Methods

Location and Sampling Scheme

In 2023, FPV arrays (70% aerial coverage) were deployed on three ponds at the Cornell Experimental Ponds Facility in Ithaca, New York, USA (42.5049 N, 76.4666 W). The experiment used a before-after-control-impact design, with observational sampling of six ponds starting in 2022 with FPV deployment in 2023 (Ray et al. 2024). The ponds are 30 x 30 m inverted, truncated pyramids, 1.75 m deep, unlined, with sediment accumulation since their construction in 1958-1959. Rooted, submerged macrophytes dominate primary production.

We returned in summer 2024 to continue measurements of dissolved CH_4 (surface and bottom), temperature, and dissolved oxygen (4 depths; 0.1, 0.75, 1, and 1.25 m from the water surface). We sampled CH_4-cycling microbes four times in 2024 from surface water, bottom water, and sediments. On July 11, 2024, we measured diffusive CH_4 exchange and net CH_4 production or consumption in surface waters, bottom waters, and sediments.

Observational CH_4 Concentration Measurements

We collected samples to determine dissolved CH_4 concentrations in the surface and bottom water of each pond six times between June 20 and September 5. Samples were collected in triplicate from the pond center using a headspace equilibration approach, with surface samples collected by hand at 10 cm depth and bottom water collected using a Van-Dorn bottle ~10 cm from the sediment-water interface (Ray et al. 2024). Samples were stored in 12 mL pre-evacuated borosilicate exetainers until analysis using a gas chromatograph equipped with a flame ionization detector (Shimadzu GC-2014).

Microbial Sample Collection and Preservation

Water samples for microbial analysis were collected as for CH_4 measurements and sequentially filtered through 200 µm and 20 µm NYTEX mesh into 2 L Nalgene bottles and kept on ice until return to the lab the same day. Surface sediments (top 2 cm) were collected using a PVC pole corer and stored in WhirlPak bags in the cooler. Water was filtered onto 0.22 µm polyethersulfone filters using a peristaltic pump (190-2020 mL per sample). Sediments were homogenized using a stainless-steel coffee grinder (three 1 second pulses per sample). Filters

70 (halved) and homogenized sediment were stored in 2 mL cryovials at -80 °C. Samples were fixed
71 with 1 µL 25% glutaraldehyde, diluted 15–20×, stained with SYBR Green I, and run in triplicate
72 on an Attune NxT (*see supplemental methods*).
73
74 **Microbial DNA Extraction, Sequencing and Bioinformatics**
75 DNA was extracted from half filters using the DNeasy PowerWater Kit and from sediments
76 using the DNeasy PowerSoil Pro Kit (Qiagen), eluted in 50 µL elution buffer, quantified
77 with a Qubit fluorometer (Thermo-Fisher) and stored at −20 °C. The V4 region of the 16S
78 rRNA gene was amplified following the Earth Microbiome Project protocols (Caporaso et al.
79 2011; Apprill et al. 2015; Parada et al. 2016) using triplicate 25 µL PCRs with KAPA HiFi 2X
80 Mastermix (Roche), 0.2 µM 515F (5'-GTGYCAGCMGCCGCGGTAA) and 806R (5'-
81 GGACTACNVGGGTWTCTAAT) primers with Illumina Nextera overhangs, and 5 ng template
82 DNA. Zymo-BIOMICS Microbial Community DNA Standard (Zymo) was included to assess
83 error rates. Samples, including PCR and indexing blanks, were pooled, indexed, and sequenced
84 (2 x 250 bp) on an Illumina MiSeq sequencer at the Cornell Biotechnology Resources Center.
85
86 Raw sequences were processed into amplicon sequence variants (ASVs) using the DADA2
87 workflow (Callahan et al. 2016) in R. Reads were trimmed to 253-254 base pairs (max error = 1),
88 merged, denoised, and chimera-checked. Taxonomy was assigned with GreenGenes2 (McDonald
89 et al. 2024). Data were imported into *phyloseq* (McMurdie and Holmes 2013); mitochondrial,
90 chloroplast, and ASVs with a higher relative abundance in blanks were removed. The mock
91 community revealed 27 spurious ASVs (error rate of 0.099%). Samples with low read counts
92 were excluded, resulting in 8,188-171,275 reads per sample. Water column ASV relative

abundances were multiplied by cell counts to obtain absolute ASV counts per mL whereas the ASV relative abundances in sediments were multiplied by the minimum library size (20,822 sequences) for relative abundance.

Microbial metabolic profiles were predicted using Functional Annotation of Prokaryotic Taxa (FAPROTAX) based on cultured prokaryotes (Louca et al. 2016). Methanogens and methanotrophs were identified at the order level and verified through literature and public databases (NCBI; Table S6).

Diffusive CH_4 Flux Measurements and Estimation of k600

We measured diffusive fluxes at the center and edge of each pond using floating chambers (18.93 L volume; 0.071 m^2 cross sectional area) attached to a portable analyzer that determines CH_4 concentrations in air using off-axis integrated cavity output spectroscopy (GLA132-GGA, ABB Measurement and Analytics; Ray et al. 2024). At the same time, we collected headspace samples for determination of dissolved CH_4 concentrations. Using diffusive CH_4 flux measurements and dissolved CH_4 concentrations, we calculated gas transfer velocities.

Water Column CH_4 Bottle Incubations

We used light and dark bottle incubations to determine rates of CH_4 production and consumption in surface and bottom waters of each pond. Immediately following the collection of dissolved CH_4 samples, we filled 125 mL glass incubation bottles (one clear and one darkened with electrical tape) and sealed them with a gas tight rubber septa. These bottles were then suspended either 10 cm from the surface or 10 cm from the sediment-water interface. The following day,

bottles were collected, de-capped, and sampled for temperature, dissolved oxygen, and dissolved CH_4 concentrations collected as described previously. Rates of CH_4 production or consumption were then calculated as the change in dissolved CH_4 concentration over time, assuming starting conditions in each bottle matched the conditions in the pond when the bottles were filled.

Sediment CH_4 Bottle Incubations

We collected sediments alongside microbial samples and stored in acid-washed polyethylene bottles at −20 °C. To determine rates of potential sediment CH_4 production, we performed bench-top bottle incubations. We added ~ 5 g wet weight of thawed sediment to 125 mL glass incubation bottles equipped with optical O_2 sensor spots (FireSting -GO2, PyroScience GMBH), added 70 mL of tap water that had been left out for > 24 hrs, sealed the vials with gas tight rubber septa, and then over-pressured each vial with 15 mL of lab air. Two replicate bottles were used per pond. Samples for analysis of headspace CH_4 concentration were collected on day 0, 2, 5, 6, and 14 by collecting 3ml headspace in 2.5 mL gas-tight vials, analyzed as described previously. Incubations were performed in the dark with room temperature ~22 °C. To compare sediment CH_4 production potential, we calculated rates of sediment CH_4 production over time relative to the dry mass of sediment in each bottle.

Statistical Comparisons

All statistical analyses were performed using R statistical software and figures were made using the *ggplot2* package (Wickham 2016). We considered the results of statistical tests to be significant when $p < 0.05$.

We fit linear mixed-effects models (fixed: treatment, day of year; random: pond) to compare environmental and microbial metrics in FPV compared to control ponds using *lme4* (Bates et al. 2015; Table S1). Rates of water column CH_4 production or consumption in surface and bottom waters were compared using a mixed effects model of light or dark bottle and FPV presence with pond as a random effect (Table S2). Contrasts between treatments were made using least square means tests via *emmeans* (Lenth 2018) (Table S3).

Water temperature and oxygen were depth-averaged by pond and day. Diffusive CH_4 fluxes, k600, and potential sediment CH_4 production were compared using two-tailed t-tests (Tables S4–S5).

Bray–Curtis dissimilarities were visualized with PCoA and tested using PERMANOVA (adonis2) and β-dispersion (betadisper) in *vegan* (Oksanen et al. 2018). Water column ASVs were scaled to total cell counts; sediment ASVs were rarefied. Differentially abundant ASVs were identified with ANCOMBC-II (tax_level = "ASV"; prevalence >10%, hol-adjusted $q < 0.05$, global test by FPV; Lin and Peddada 2024).

Results

FPV Ponds were Colder and Less Oxygenated

Ponds with FPV were on average almost 4 °C colder across the water column (18.87 ± 1.69 °C; mean ± SD) than control ponds (22.78 ± 2.29 °C) during summer ($p < 0.001$; Fig. S1). While all ponds were generally undersaturated in DO, surface waters in control ponds were occasionally oversaturated, unlike FPV ponds, which remained undersaturated throughout (Fig. S2). Mean

DO in FPV ponds (30.18 ± 10.59 %) was less than half that of control ponds (62.34 ± 10.59 %; $p < 0.001$).

FPV Ponds had Higher CH_4 Concentrations at Depth

Dissolved CH_4 concentrations were relatively stable over time (Fig. 3A & 3C). Surface CH_4 did not differ between FPV (1.79 ± 4.01 µmol CH_4 L^{-1}) and control ponds (2.07 ± 3.19 µmol CH_4 L^{-1}; $p = 0.208$; Fig. 3B). However, bottom water CH_4 was two orders of magnitude higher than in surface waters, and more than twice as high in FPV ponds (306.2 ± 419.0 µmol CH_4 L^{-1}) than controls (129.7 ± 45.60 µmol CH_4 L^{-1}; $p = 0.003$; Fig. 3D).

FPV Increased Late-Summer Methanotroph Abundance in the Water Column

CH_4 associated microbial abundance differed between FPV and control ponds, driven primarily by increases in water column methanotrophs in late-summer. In surface waters, methanotroph abundance increased throughout summer and was five times higher in FPV ponds (4.6 ± 4.6 x 10^5 cells mL^{-1}) than controls (0.9 ± 0.9 x 10^5 cells mL^{-1}; $p < 0.001$; Fig. 2A-B). Methanogen abundance was orders of magnitude lower and showed no surface water differences between treatments (Fig. 2C & D). Bottom waters displayed similar trends, with 3.5 times more methanotrophs in FPV ponds (Fig. 2E-H). In contrast, sediment methanogens averaged ~20% of the community and were more abundant than methanotrophs, (~5%), but neither group differed between treatments (Fig. 2I-L).

FPV Altered CH_4-Cycling Communities

184 FPV significantly altered CH_4-cycling communities in both water and sediment (Fig. 3; Table 1).
185 In the water column, FPV had the strongest effect (pseudo-F = 8.20; R^2 = 0.11), while pond
186 explained slightly more variance (R^2 = 0.13) but caused less separation (pseudo-F = 2.40). Day
187 of year also contributed to variation (R^2 = 0.10). In sediments, pond was the dominant driver of
188 community change (pseudo-F = 4.53; R^2 = 0.24), but FPV still induced clear shifts (pseudo-F =
189 8.41; R^2 = 0.11), with additional variance explained by day of year (R^2 = 0.08).
190
191 Taxon-specific analyses revealed similar patterns (Fig.S3A&B; Table S7): pond identity
192 dominated methanogen community structure (R^2 = 0.28), while FPV exerted stronger effects on
193 methanotrophs (pseudo-F = 7.69; R^2 = 0.10) than on methanogens (pseudo-F = 10.47; R^2 = 0.12)
194 (Table S7). FPV effects were most pronounced in the water column, likely driven by
195 methanotrophs given the absence of methanogens, while sediment communities reflected
196 stronger spatial structuring.
197
198 **Type I Methanotrophs Drove CH_4 Cycler Community Change**
199 Four methanotrophic ASVs were higher in the water column of FPV ponds compared to
200 controls: from Methylococcaceae (*Methyloparacoccus)* and Methylomondadaceae
201 (*Methylobacter_C*, *Methylococcales*, *Methylomonas*) (Fig. 4). Methyloparacoccus reached
202 densities over 500,000 cells/mL ($p < 0.001$). The only enriched methanogen,
203 *Methanobacterium_B* , was present at lower abundances (<10,000 cells/mL; p = 0.037). Only
204 one differentially abundant ASV was detected in the sediments, Methanoperedens_A
205 (ASV_4603; a methanogen), but its relative abundance was negligible.
206

No Apparent Differences in CH_4 Cycling Processes

We found no differences in diffusive water-air CH_4 exchange or gas transfer velocities between ponds with and without FPV or between the center and edge of ponds (Table S4). On average, all ponds emitted CH_4 to the atmosphere at a rate of 404.1 ± 896.6 µmol CH_4 m^{-2} h^{-1}. We also found no difference in rates of water column CH_4 net-production or consumption between ponds with and without FPV (Table S3). Sediments from both open and FPV ponds produced CH_4, but we found no difference in potential CH_4 production by sediments in ponds with FPV (5.43 ± 4.81 ppm CH_4 g dry $sediment^{-1}$ d^{-1}) compared to those without (14.13 ± 10.92 ppm CH_4 g dry $sediment^{-1}$ d^{-1}; $p = 0.303$; Table S5).

Discussion

We found that dissolved CH_4 concentrations remain elevated in bottom waters for two years following FPV deployment (Fig. 1D) and water column methanotroph abundance is enhanced in ponds with FPV (Fig. 2). Surface water CH_4 – and diffusive CH_4 emissions – were similar between FPV and control ponds. Taken together, this decoupling suggests that FPV induced changes to redox conditions allows for a buildup of CH_4 in bottom-waters, but biological responses limit CH_4 flux to the atmosphere.

Specifically, we hypothesize that lower oxygen conditions in FPV ponds prolong anoxic conditions, allowing for greater CH_4 accumulation at depth. These shifted redox conditions allow for sustained CH_4 production in sediments and accumulation of CH_4 in waters overlying the sediments. A persistently large CH_4 pool likely fuels type I methanotrophy in the water column where oxygen is more available. Methanotrophs reached bloom-like densities in late summer,

230 exceeding one million cells per milliliter and reaching levels ten times higher in FPV than
231 controls (Fig 2A). By intercepting CH_4 near the air-water interface, methanotrophs likely reduce
232 CH_4 concentrations before atmospheric release.
233
234 Beyond CH_4 availability, changes in microbial community composition also likely reflect shifts
235 in redox conditions under FPV-driven hypoxia. For example, several *Methylomonadaceae* taxa
236 were more abundant in FPV ponds. These type I CH_4-oxidizing bacteria are adapted to low-
237 oxygen environments and high CH_4 availability (Li et al. 2024). Type I methanotrophs use the
238 ribulose monophosphate (RuMP) pathway for carbon assimilation, which is more energy
239 efficient than the serine pathway used by Type II methanotrophs and supports faster growth rates
240 under high CH_4 conditions (Knief, 2015). Notably, methanotrophs are rarely measured in
241 freshwater CH_4 studies (Wang et al., 2021) and our results highlight the importance of examining
242 both CH_4 producers and consumers to understand how engineered systems influence microbial
243 CH_4 cycling. Whole-community perspectives also reveal how broader microbial assemblages
244 mediate CH_4 production responses (Bertolet et al. 2022).
245
246 By pairing amplicon sequencing with flow cytometry, we move beyond relative abundance to
247 quantify absolute abundance of CH_4 cycling taxa in the water column. In late summer,
248 methanotrophs surpassed one million cells mL^{-1} in FPV surface waters – a density rarely
249 reported in any aquatic system. This bloom may reflect the metabolic advantage of Type I
250 methanotrophs under CH_4 -rich, low-O_2 conditions. While activity remains to be directly
251 measured, these abundances suggest strong microbial capacity to intercept CH_4 before it reaches
252 the atmosphere. This integrative approach lays essential groundwork for predicting how

microbial communities mediate greenhouse gas fluxes under engineered shading. As FPV deployment expands, incorporating microbial responses into biogeochemical assessments will be critical for managing the climate impacts of aquatic renewable energy.

Our results also demonstrate that the effect of FPV on pond biogeochemistry and CH_4 cycling varies over time. Immediately following FPV deployment in 2023, FPV ponds had lower oxygen concentrations and increased surface and bottom water CH_4 concentrations (Ray et al. 2024). By contrast, in the second year (2024), surface CH_4 concentrations no longer differed between treatments, and methanotroph abundance was substantially higher in FPV surface waters. These patterns suggest a time-lagged ecological response, where sustained hypoxia promotes bottom-water CH_4 accumulation, followed by methanotroph enrichment that buffers CH_4 flux near the surface. Quantifying how CH_4 ebullition responds to FPV deployment across seasons and years remains a key open question for understanding total emission dynamics.

Identifying strategies for low emission energy production is critical for combating climate change. As FPV expansion accelerates, understanding how this technology interacts with aquatic CH_4 dynamics is important for ensuring sustainability. Our study provides mechanistic evidence that FPV deployment can restructure microbial communities in ways that influence carbon cycling, offering a foundation for evaluating the long-term ecosystem-level impacts of continued FPV proliferation.

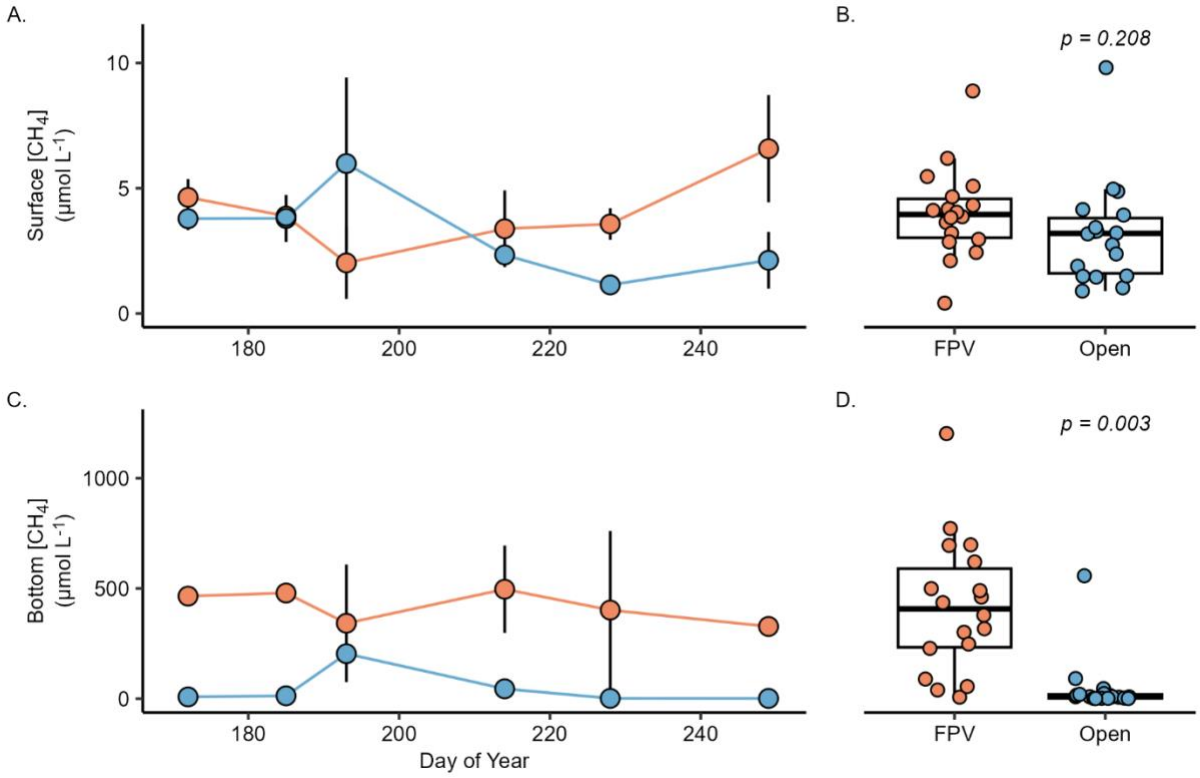

Fig. 1: Dissolved methane concentrations in the surface (A, B) and bottom water (C, D) of ponds with and without floating photovoltaic (FPV) arrays in summer 2024. In (A, C) points indicate the mean CH_4 concentration from pond centers on a given date by treatment group and error bars indicate standard deviation. Colored lines connect the means. In panels (B, D) each point on the boxplot indicates a measured CH_4 concentration in an individual pond based on whether FPV is present (FPV) or not (Open) and p-values indicate the result of a least-squares mean test of the treatment effect of the mixed model (Table S3).

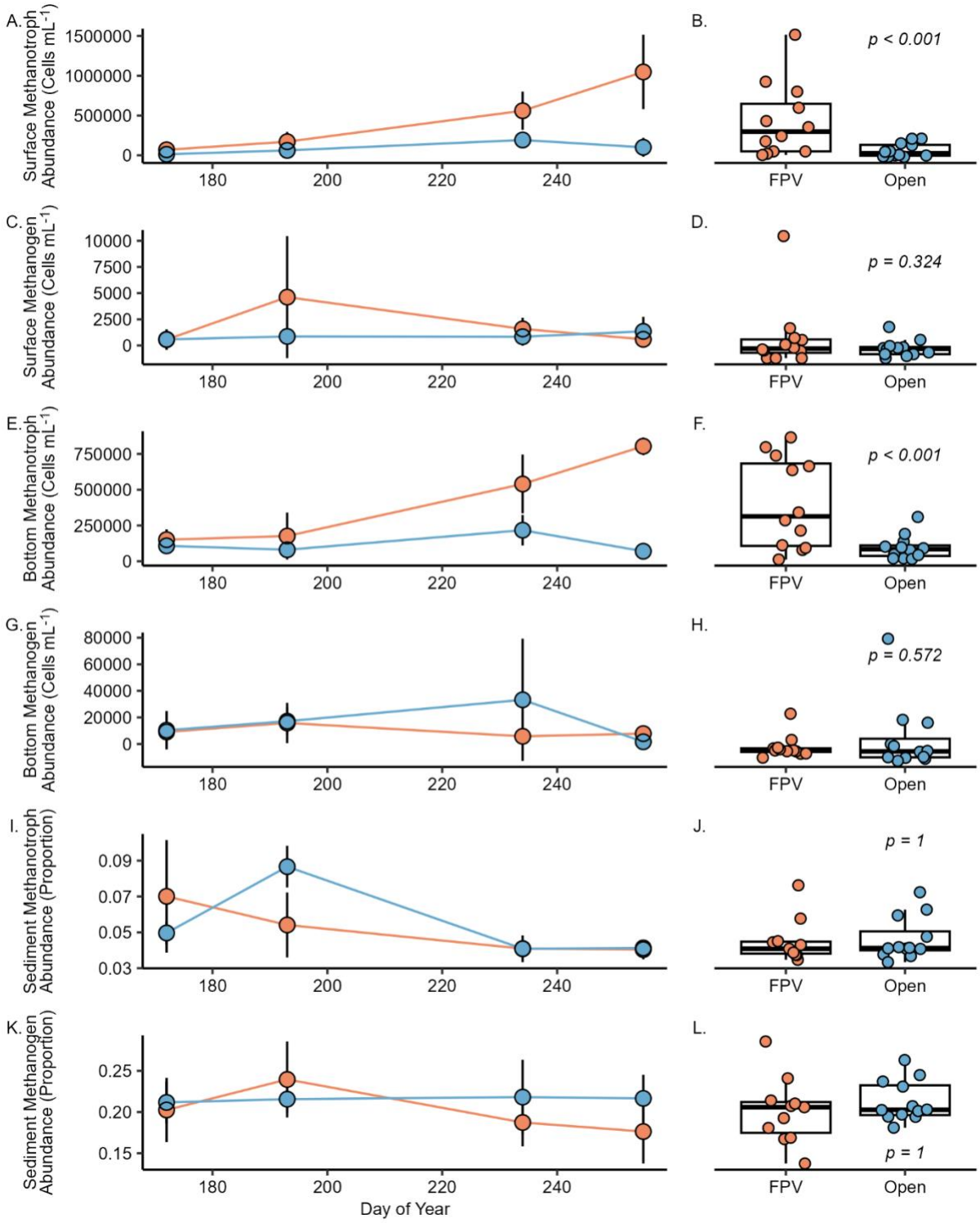

Fig. 2: Total abundance (A-H) of methanogens and methanotrophs in surface waters and bottom waters and relative abundance (I-L) of methanogens and methanotrophs in sediments of ponds with and without floating photovoltaic (FPV) arrays in summer 2024. Information as for Fig. 2.

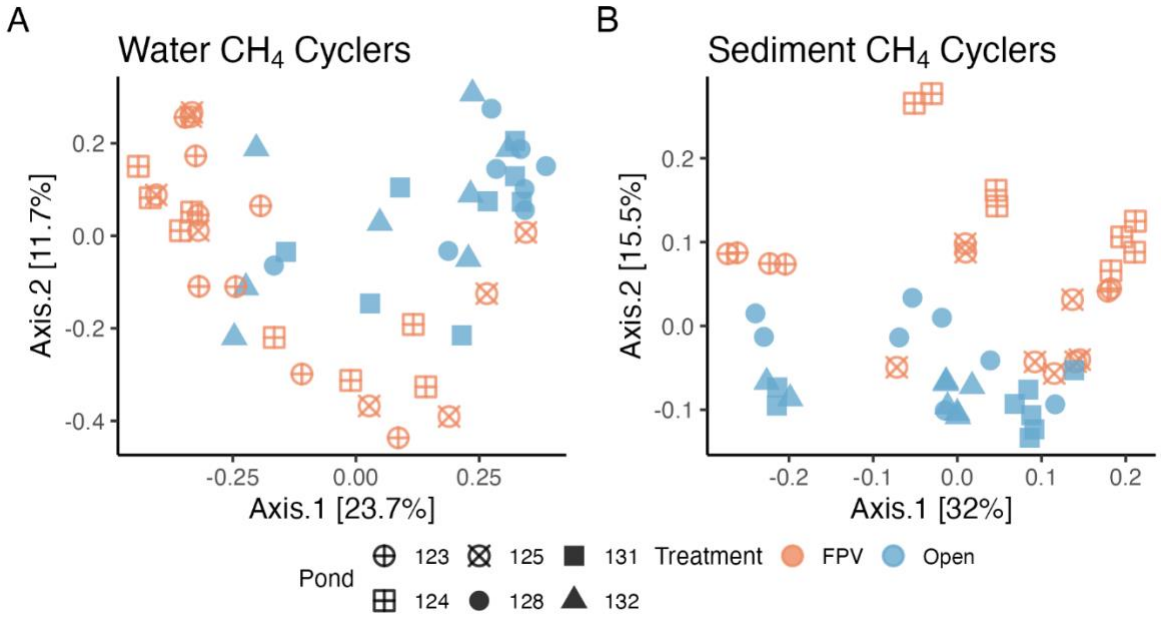

Fig. 3: Bray–Curtis PCoA of combined methanogen and methanotroph communities in ponds with floating photovoltaic arrays ("FPV") and control ponds ("Open"). (A) Dissimilarity among water column samples was calculated using absolute cell abundances. (B) Sediment samples were rarefied to 20,822 reads to calculate dissimilarity based on relative abundance; replicates are shown separately. Shapes denote ponds. PERMANOVA and beta dispersion statistics are in Table 1.

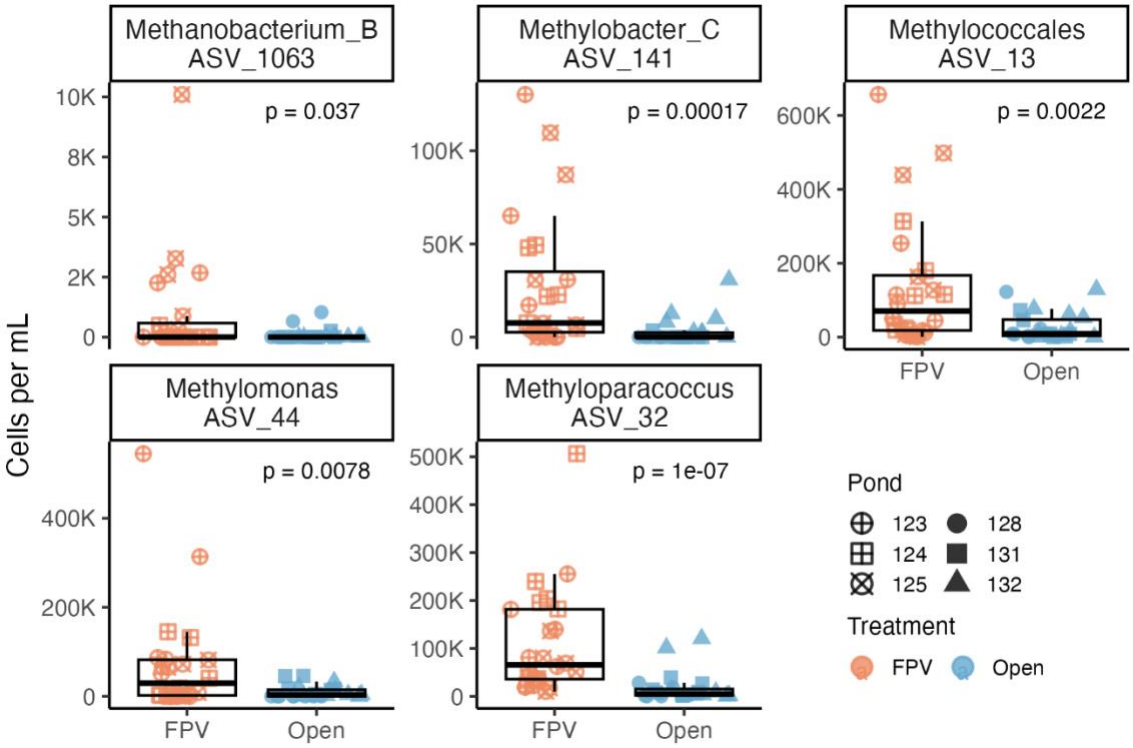

Fig. 4: Absolute cell abundances (cells mL^{-1}) of five differentially abundant ASVs identified by ANCOM-BC II in the water column of ponds with floating photovoltaic arrays ("FPV") and control ponds without FPV ("Open"). ASV_1063 (Methanobacterium_B) is a methanogen; the remaining ASVs represent Type I methanotrophs. Shapes indicate individual ponds. All comparisons are between FPV and open ponds. P-values reflect Wilcoxon rank-sum tests.

Table 1: FPV treatment, pond, and DOY significantly influence methane-cycling community composition. PERMANOVA and β-dispersion results for CH_4-cycling communities in water and sediment samples from FPV and control ponds. Bray-Curtis dissimilarities were calculated using absolute abundances for water (Fig. 3A) and rarefied relative abundances for sediment (Fig. 3B). PERMANOVA tested effects of FPV, pond, and day of year (DOY) and their interactions; β-dispersion tested group variance. Residual R^2 shown for each habitat.

Habitat Type	CH_4 Group	Variable	PERMANOVA				®-Dispersion		Figure
			R^2	Pseudo-F	p-value	Residuals	F	p-value	
Water	All	FPV	0.11381	8.2023	0.001	0.49950	7.5386	0.011	3A
Water	All	Pond	0.13354	2.4061	0.001		1.3603	0.256	3A
Water	All	DOY	0.09599	6.9181	0.001		4.8804	0.006	3A
Water	All	FPV:DOY	0.07641	5.5072	0.001				3A
Water	All	Pond:DOY	0.08075	1.4549	0.034				3A
Sediment	All	FPV	0.11101	8.4062	0.001	0.44900	0.3718	0.673	3B
Sediment	All	Pond	0.23926	4.5295	0.001		0.1485	0.835	3B
Sediment	All	DOY	0.07753	5.8706	0.001		1.7651	0.162	3B
Sediment	All	FPV:DOY	0.02773	2.0998	0.018				3B
Sediment	All	Pond:DOY	0.09548	1.8074	0.005				3B

Acknowledgements
This work was supported by an Atkinson Academic Venture Fund to SMG, MAH, MLS, awards 441993/2023-0 and 200781/2024-3 from National Council for Scientific and Technological Development (CNPq) to SJC, and startup funds from the University of Delaware made available to NER. We thank Benj Sterrett for helping to maintain access to the ponds, Autumn Newman, Gus Pendleton, Sophia Richter and Kailyn Hanke for assistance with field and lab work, and Jera Jansen, Caitlin Davis, Mônica Antunes-Ulyssea, Sheena Dwyer-McNulty, Trifosa Simamora, Tim Boycott, and Dave Grodsky for helping construct the floating solar arrays.

References

Aben, R. C. H. and others. 2017. Cross continental increase in methane ebullition under climate change. Nat Commun **8**: 1682. doi:10.1038/s41467-017-01535-y

Almeida, R. and others. 2022. Floating solar power: evaluate trade-offs. Nature **606**: 246–249.

Andini, S., N. Suwartha, E. A. Setiawan, and S. Ma'arif. 2022. Analysis of biological, chemical, and physical parameters to evaluate the effect of floating solar PV in Mahoni Lake, Depok, Indonesia: Mesocosm experiment study. Journal of Ecological Engineering **23**: 201–207. doi:10.12911/22998993/146385

Apprill, A., S. Mcnally, R. Parsons, and L. Weber. 2015. Minor revision to V4 region SSU rRNA 806R gene primer greatly increases detection of SAR11 bacterioplankton. Aquatic Microbial Ecology **75**: 129–137. doi:10.3354/ame01753

Bastviken, D., J. Cole, M. Pace, and L. Tranvik. 2004. Methane emissions from lakes: Dependence of lake characteristics, two regional assessments, and a global estimate. Global Biogeochem Cycles **18**: 1–12. doi:10.1029/2004GB002238

Bates, D., M. Maechler, B. Bolker, and S. Walker. 2015. Fitting linear mixed-effects models using *lme4*. J Stat Softw **67**: 1–48. doi:10.1126/science.1176170

Bertolet, B. L., C. Koepfli, and S. E. Jones. 2022. Lake Sediment Methane Responses to Organic Matter are Related to Microbial Community Composition in Experimental Microcosms. Front Environ Sci **10**. doi:10.3389/fenvs.2022.834829

Callahan, B. J., P. J. McMurdie, M. J. Rosen, A. W. Han, A. J. A. Johnson, and S. P. Holmes. 2016. DADA2: High-resolution sample inference from Illumina amplicon data. Nat Methods **13**: 581–583. doi:10.1038/nmeth.3869

Caporaso, J. G., C. L. Lauber, W. A. Walters, D. Berg-Lyons, C. A. Lozupone, P. J. Turnbaugh, N. Fierer, and R. Knight. 2011. Global patterns of 16S rRNA diversity at a depth of millions of sequences per sample. Proc Natl Acad Sci U S A **108**: 4516–4522. doi:10.1073/pnas.1000080107

Cazzaniga, R., and M. Rosa-Clot. 2021. The booming of floating PV. Solar Energy **219**: 3–10. doi:10.1016/j.solener.2020.09.057

Dörenkämper, M., A. Wahed, A. Kumar, M. de Jong, J. Kroon, and T. Reindl. 2021. The cooling effect of floating PV in two different climate zones: A comparison of field test data from the Netherlands and Singapore. Solar Energy **219**: 15–23. doi:10.1016/j.solener.2021.03.051

Gallaher, A., E. L. Kalies, and S. M. Grodsky. 2025. Sustainability trade-offs across modeled floating solar waterscapes of the Northeastern United States. Cell Reports Sustainability. doi:10.1016/j.crsus.2025.100423

Ilgen, K., D. Schindler, S. Wieland, and J. Lange. 2023. The impact of floating photovoltaic power plants on lake water temperature and stratification. Sci Rep **13**. doi:10.1038/s41598-023-34751-2

Jackson, R. B. and others. 2024. Human activities now fuel two-thirds of global methane emissions. Environmental Research Letters **19**: 101002. doi:10.1088/1748-9326/ad6463

Jin, Y. and others. 2023. Energy production and water savings from floating solar photovoltaics on global reservoirs. Nat Sustain **6**: 865–874. doi:10.1038/s41893-023-01089-6

Knief, C. 2015. Diversity and habitat preferences of cultivated and uncultivated aerobic methanotrophic bacteria evaluated based on *pmoA* as molecular marker. Frontiers in Microbiology **6**: 1346.

Lenth, R. 2018. *emmeans*: Estimated marginal means, aka least-squares means. R package version 1.2.3.

Li, B., Z. Mao, J. Xue, P. Xing, and Q. L. Wu. 2024. Metabolic versatility of aerobic methane-oxidizing bacteria under anoxia in aquatic ecosystems. Environmental Microbiology Reports **16**. doi:10.1111/1758-2229.70002

Lin, H., and S. Das Peddada. 2024. Multigroup analysis of compositions of microbiomes with covariate adjustments and repeated measures. Nat Methods **21**: 83–91. doi:10.1038/s41592-023-02092-7

Louca, S., L. Parfrey, and M. Doebeli. 2016. Decoupling function and taxonomy in the global ocean microbiome. Science (1979) **353**: 1272–1277. doi:10.1126/science.aad8279

McDonald, D. and others. 2024. Greengenes2 unifies microbial data in a single reference tree. Nat Biotechnol **42**: 715–718. doi:10.1038/s41587-023-01845-1

McMurdie, P. J., and S. Holmes. 2013. Phyloseq: An R Package for Reproducible Interactive Analysis and Graphics of Microbiome Census Data. PLoS One **8**: e61217. doi:10.1371/journal.pone.0061217

Nobre, R., S. M. Rocha, S. Healing, Q. Ji, S. Boulêtreau, A. Armstrong, and J. Cucherousset. 2024. A global study of freshwater coverage by floating photovoltaics. Solar Energy **267**. doi:10.1016/j.solener.2023.112244

Oksanen, J. and others. 2018. *vegan*: Community Ecology Package. R package version 2.5.

Parada, A. E., D. M. Needham, and J. A. Fuhrman. 2016. Every base matters: Assessing small subunit rRNA primers for marine microbiomes with mock communities, time series and global field samples. Environ Microbiol **18**: 1403–1414. doi:10.1111/1462-2920.13023

R Core Team. 2014. R: A language and environment for statistical computing.

Ramanan, C. J., K. H. Lim, J. C. Kurnia, S. Roy, B. J. Bora, and B. J. Medhi. 2024. Towards sustainable power generation: Recent advancements in floating photovoltaic technologies. Renewable and Sustainable Energy Reviews **194**: 114322. doi:10.1016/j.rser.2024.114322

Ray, N. E., and M. A. Holgerson. 2023. High intra-seasonal variability in greenhouse gas emissions from temperate constructed ponds. Geophys Res Lett **50**: e2023GL104235. doi:10.1029/2023GL104235

Ray, N. E., M. A. Holgerson, and S. M. Grodsky. 2024. Immediate Effect of floating solar energy deployment on greenhouse gas dynamics in ponds. Environ Sci Technol **58**: 22104–22113. doi:10.1021/acs.est.4c06363

Wang, B., E. Stirling, Z. He, B. Ma, H. Zhang, X. Zheng, F. Xiao, and Q. Yan. 2021. Pollution alters methanogenic and methanotrophic communities and increases dissolved methane in small ponds. Science of the Total Environment **801**. doi:10.1016/j.scitotenv.2021.149723

Wang, T. W. and others. 2022. Effects of floating photovoltaic systems on water quality of aquaculture ponds. Aquac Res **53**: 1304–1315. doi:10.1111/are.15665

Wickham, H. 2016. *ggplot2*: Elegant Graphics for Data Analysis, Springer-Verlag.

Woolway, R. I., G. Zhao, S. M. G. Rocha, S. J. Thackeray, and A. Armstrong. 2024. Decarbonization potential of floating solar photovoltaics on lakes worldwide. Nature Water **2**: 566–576. doi:10.1038/s44221-024-00251-4